Boletín de la Sociedad Española de Cerámica y Vidrio
Vol 53, 4, 207-212, Julio-Agosto 2014 ISSN 0366-3175. eISSN 2173-0431.
http://dx.doi.org/10.3989/cyv.242014

BOLETIN DE LA SOCIEDAD ESPAÑOLA DE
Cerámica y Vidrio
A R T I C U L O

Processing effects on the thermoelectric properties of $Bi_2Ca_2Co_{1.7}O_x$ ceramics

SH. RASEKH[1]*, G. CONSTANTINESCU[1], M. A. MADRE[1], M. A. TORRES[2], J. C. DIEZ[1] AND A. SOTELO[1]

[1]Instituto de Ciencia de Materiales de Aragón (CSIC-Universidad de Zaragoza), Mª de Luna 3, 50018 Zaragoza, Spain.
[2]Departamento de Ingeniería de Diseño y Fabricación. Universidad de Zaragoza, Mª de Luna, 3. 50018 Zaragoza, Spain.
*Corresponding author: Sh. Rasekh. E-mail: sh.rasekh@unizar.es
Address: Dept. Ciencia de Materiales; C/Mª de Luna, 3; 50018-Zaragoza; Spain
Tel: +34 976762617. Fax: +34 976761957

$Bi_2Ca_2Co_{1.7}O_x$ bulk polycrystalline ceramics were prepared by the solid state method and by directional growth. Moreover, the effect of annealing on the textured materials has been studied. Microstructure has shown randomly oriented grains in the classical sintered materials while in the textured samples those were well oriented with their c-axis nearly perpendicular to the growth direction. Furthermore, the textured-annealed samples showed much lower amount of secondary phases than the as-grown ones. These microstructural changes are reflected on the thermoelectric properties which increase with the grain orientation and with the decrease on the secondary phase content mainly due to the electrical resistivity reduction. As a consequence, a raise on the power factor of about 6 and 9 times, compared with the classically sintered samples, was obtained for the as-grown and textured-annealed ones, respectively. The maximum power factor obtained at 650 ºC in the textured-annealed samples (~ 0.31 mW/K²m) is about 50 % higher, at the same temperature, than the obtained in one of the most used methods for texturing this kind of materials, the sinter-forging process.

Keywords: Sintering; Texturing; Cobaltites; Electrical properties; Thermopower.

Efecto del procesado en las propiedades termoeléctricas de materiales cerámicos $Bi_2Ca_2Co_{1.7}O_x$

Se han preparado cerámicas policristalinas volumétricas de $Bi_2Ca_2Co_{1.7}O_x$ por medio del método clásico de estado sólido y por crecimiento direccional. Además, se ha estudiado el efecto del recocido en los materiales texturados. La microestructura ha mostrado granos orientados al azar en las muestras preparadas por sinterizado en estado sólido, mientras que en las muestras texturadas se orientaban con el eje c perpendicular a la dirección de crecimiento. Por otro lado, las muestras texturadas-recocidas mostraban una cantidad mucho menor de fases secundarias que las crecidas. Estos cambios en la microestructura se reflejan en las propiedades termoeléctricas, que aumentan con la orientación de los granos y con la disminución del contenido en fases secundarias, principalmente por la reducción en los valores de la resistividad eléctrica. Como consecuencia, se han producido aumentos del factor de potencia entre 6 y 9 veces los valores obtenidos en las muestras sinterizadas, en las crecidas y texturadas-recocidas, respectivamente. El máximo valor del factor de potencia se ha obtenido a 650 ºC en las muestras texturadas-recocidas (~ 0.31 mW/K²m), que es alrededor del 50 % mayor, a la misma temperatura, del que se ha obtenido en muestras procesadas por forjado en caliente, que es uno de los procesos más utilizados para texturar este tipo de materiales.

Palabras clave: Sinterizado; Texturado; Cobaltitas; Propiedades electricas; Termopower.

Cómo citar este artículo: Rasekh, SH.; Constantinescu, G.; Madre, M. A.; Torres, M. A.; Díez, J. C.; Sotelo, A. (2014): Processing effects on the thermoelectric properties of $Bi_2Ca_2Co_{1.7}O_x$ ceramics, *Bol. Soc. Esp. Ceram. Vidr.*, 53 (4): 207-212. http://dx.doi.org/10.3989/cyv.242014

1. INTRODUCTION

Thermoelectric (TE) materials can convert a temperature gradient to electrical power directly due to the well-known Seebeck effect. The conversion efficiency of such materials is usually quantified by the dimensionless figure of merit ZT, $TS^2/\rho\kappa$ (in which S^2/ρ is also called power factor, PF), where S is the Seebeck coefficient (or thermopower), ρ the electrical resistivity, κ the thermal conductivity, and T is the absolute temperature [1]. This important characteristic has focused attention on this type of materials in order to be used in practical applications as waste heat recovery devices [2] or solar thermoelectric generators [3]. Furthermore, they can also be used as heating/refrigeration devices [4]. Nowadays, these commercial applications are based on the use of alloys and/or intermetallic thermoelectric materials, such as Bi_2Te_3 or $CoSb_3$, with high thermoelectric performances at relatively low temperatures. On the other hand, these materials possess some drawbacks, as they can be degraded at high temperatures under air and/or releasing toxic or heavy elements. These problems lead to the limitation of their working temperature which reduces their effective performances, as can be deduced from the ZT expression.

This temperature limitation was overwhelmed in 1997 by the discovery of attractive thermoelectric properties in the $NaCo_2O_4$ ceramic [5]. Since the discovery of this thermoelectric oxide, much work has been performed on the cobaltite ceramics as promising thermoelectric materials for high temperature applications. The intense research work continues on Co-oxide based materials, such as $Ca_3Co_4O_9$, $LaCoO_3$, $Bi_2Sr_2Co_2O_9$ and $Bi_2Ca_2Co_2O_y$ with interesting thermoelectric properties and high working temperatures [6-9]. Moreover, these oxide materials have the great advantage of being able to operate at high temperatures in air without degradation, in comparison to the intermetallic thermoelectric compounds, which is another way for improving the ZT values.

The crystal structure of these CoO families is composed of two different layers, with an alternate stacking of a common conductive CdI_2-type CoO_2 layer with a two-dimensional triangular lattice and a block layer, composed of insulating rock-salt-type (RS) layers. The two sublattices (RS block and CdI_2-type CoO_2 layer) possess common *a*- and *c*-axis lattice parameters and β angles but different *b*-axis length, causing a misfit along the *b*-direction [10]. It has been reported that the misfit factor and/or the charge of the RS block layer between the CoO_2 ones govern the Seebeck coefficient values [11]. This characteristic provides the basis for the modification of thermoelectric properties of a given material via chemical substitutions. The most common ones substitute an alkaline-earth by a rare-earth as Yb for Ca in $Ca_3Co_4O_9$ [12], or Co by another transition metal, as Cu in $Ca_3Co_4O_9$ [13]. Other usual substitutions are Pb for Bi in $Bi_2Sr_2Co_{1.8}O_x$ [14], metallic Ag additions in $Ca_3Co_4O_9$ and $Bi_2Sr_2Co_{1.8}O_x$ [15,16], or an alkaline-earth by another one as Ca for Sr in $Bi_2Sr_2Co_{1.8}O_x$ [17].

On the other hand, as layered cobaltites are materials with a strong crystallographical anisotropy, the alignment of plate-like grains by mechanical and/or chemical processes is necessary to attain macroscopic properties comparable to those obtained on single crystals. Some techniques have been shown to be adequate to obtain a good grain orientation in several oxide ceramic systems, as Template Grain Growth (TTG) [18], Spark Plasma Sintering (SPS) [19], laser floating zone melting (LFZ) [20], or electrically assisted laser floating zone (EALFZ) [21].

The aim of the present work is studying the modification of microstructure and thermoelectric properties of $Bi_2Ca_2Co_{1.7}O_x$, comparing the classically sintered materials with the textured and textured-annealed ones.

2. MATERIALS AND METHODS

The polycrystalline $Bi_2Ca_2Co_{1.7}O_x$ ceramics used for this study have been prepared by the classical solid state route from commercial Bi_2O_3 (Panreac, 98+ %), $CaCO_3$ (Panreac, 98+ %), and Co_2O_3 (Aldrich, 98+ %) powders. They were weighed in the appropriate proportions, mixed and ball milled at 300 rpm for 30 minutes, in acetone media. The resulting suspension was placed into a glass container and dried using an infrared evaporation system. The dry powder has then been thermally treated twice at 750 and 800 ºC for about 12 hours under air, with an intermediate manual milling, in order to assure the complete decomposition of the carbonates. This thermal treatment is necessary and it has been designed specifically to avoid the presence of carbonates in the following steps. These powders were then used for the different processed samples:

a) *Classical sintering process*: The powders were uniaxially pressed at 400 MPa for 1 minute in order to obtain green ceramic parallelepipeds with an adequate size and shape for their thermoelectric characterization (~ 3 mm x 3 mm x 14 mm). These green bodies were subsequently sintered in the optimal conditions for this system, consisting in one step heating at 800 ºC for 24 h with a final furnace cooling [9].
b) *Texturing process*: The resulting powders were then cold isostatically pressed into latex tubes at ~200 MPa for around 2 minutes to obtain green ceramic cylinders which were subsequently used as feed in a LFZ device equipped with a continuous power Nd:YAG laser ($\lambda = 1.06\ \mu m$) and described elsewhere [22]. The processing of the different samples has been performed in the same conditions; they were directionally grown downwards, under air, from the melt at 30 mm/h with a seed rotation of 3 rpm. Moreover, in order to assure compositional homogeneity of the molten zone, an opposite feed rotation of 15 rpm has also been performed. Finally, after the texturing process, long (more than 15 cm) and geometrically homogeneous (~2 mm diameter) textured cylindrical rods have been produced as reported in previous works [23]. These bars were cut into pieces with the adequate dimensions for the thermoelectric characterization (~ 15 mm long).
c) *Texturing-annealing process*: Part of the samples obtained in the texturing process were subjected, after cutting, to a thermal treatment consisting in one step heating at 800 ºC for 24 h with a final furnace cooling to reduce the amount of secondary phases, as reported in previous works [24].

The identification of the main phases in all the samples was carried out using powder XRD in a Rigaku D/max-B X-ray powder diffractometer (CuKα radiation), between 10 and 70 degrees. Microstructure evolution has been observed using a scanning electron microscope (JEOL 6000) equipped with an energy dispersive X-ray spectroscopy (EDS) device, used to determine the elemental composition of the different phases. Polished sections of all samples have been observed to analyze the microstructural evolution with the different treatments. Electrical resistivity and Seebeck coefficient were simultaneously determined by the standard dc four-probe technique in a LSR3 measurement system (Linseis GmbH), in the steady state mode, at temperatures ranging from 50 to 650 ºC. With the electrical resistivity and Seebeck coefficient data, the power factor ($PF = S^2/\rho$) has been calculated in order to determine the samples performances.

3. RESULTS AND DISCUSSION

Powder XRD patterns for all the $Bi_2Ca_2Co_{1.7}O_x$ samples (from 10 to 35 degrees, for clarity), are displayed in Fig. 1. From these data, it is clear that the most intense peaks correspond to the $Bi_2Ca_2Co_{1.7}O_x$ phase (indicated by their diffraction planes in Fig. 1a), in agreement with previously published data [25]. On the other hand, peaks marked with a * in Fig. 1b correspond to the $Ca_4Bi_6O_{13}$ non-thermoelectric secondary phase [26]. When observing carefully the patterns displayed in the figure, it can be clearly seen that the number of reflections attributed to the $Bi_2Ca_2Co_{1.7}O_x$ phase

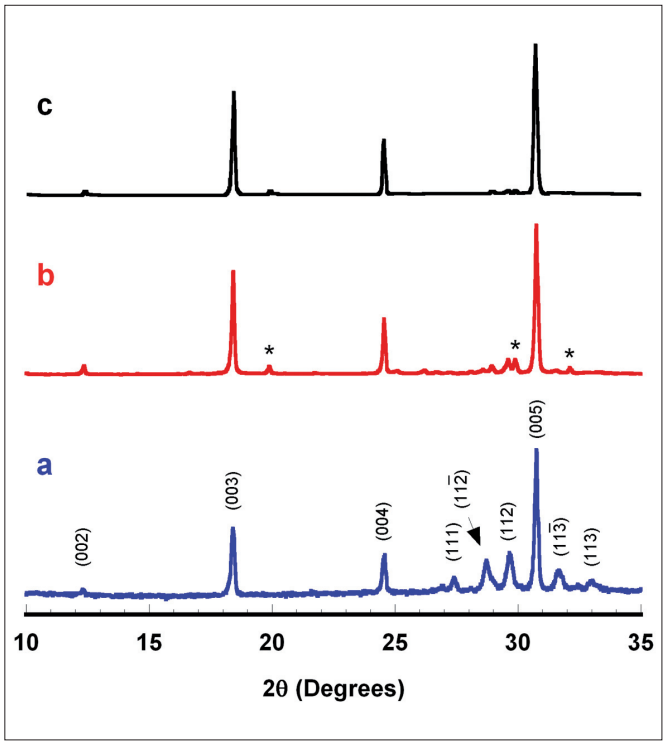

Figure 1. XRD plots of all the samples: a) classically sintered at 800 ºC for 24 h; b) as-grown textured sample; and c) textured-annealed at 800 ºC for 24 h. Crystallographic planes have been indicated on the peaks corresponding to the $Bi_2Ca_2Co_{1.7}O_y$ thermoelectric phase. * indicates the $Ca_4Bi_6O_{13}$ non-thermoelectric secondary phase.

are reduced from the samples prepared by the classical solid state method (Fig. 1a) to the textured ones (Figs. 1b and c). This effect is due to the growth of the thermoelectric grains along the ab planes which are much larger for samples textured by the LFZ technique, as reported in previous works [27]. As a consequence, these plate-like grains are preferentially oriented with their ab plane parallel to the sample holder when powdered samples are prepared for the XRD characterization. Moreover, it is also clear that the texturing process performed to the solid state prepared materials produces a higher amount of $Ca_4Bi_6O_{13}$ non-thermoelectric secondary phase, compared to the classically prepared materials, as indicated by the diffraction peaks marked by * in Fig. 1b. On the other hand, the annealing treatment is decreasing the amount of secondary phases, as can be observed by the nearly total disappearance of the peaks corresponding to the $Ca_4Bi_6O_{13}$ non-thermoelectric secondary phase (see Fig. 1c). This result clearly indicates that the temperature and time are adequate to produce nearly pure phase textured thermoelectric materials.

Representative SEM micrographs of all samples, performed on longitudinal polished samples, are shown in Fig. 2. In these micrographs it can be easily seen the microstructural evolution with the different processes. Classical sintered samples (Fig. 2a) show the thermoelectric $Bi_2Ca_2Co_{1.7}O_x$ phase (grey contrast) as the major one, together with small amounts of $Ca_4Bi_6O_{13}$ and CoO non-thermoelectric secondary phases (white and black contrasts, respectively) and some porosity. Moreover, the thermoelectric grains are randomly oriented in the whole sample volume, typical feature for the classical synthesis methods. When the samples are textured by the LFZ technique, the directional solidification produces very large and well oriented grains, growing with their c-axis nearly perpendicular to the growth direction, as illustrated in Fig. 2b. On the other hand, as already observed in similar systems [28,29] the as grown samples are composed of a mixture of

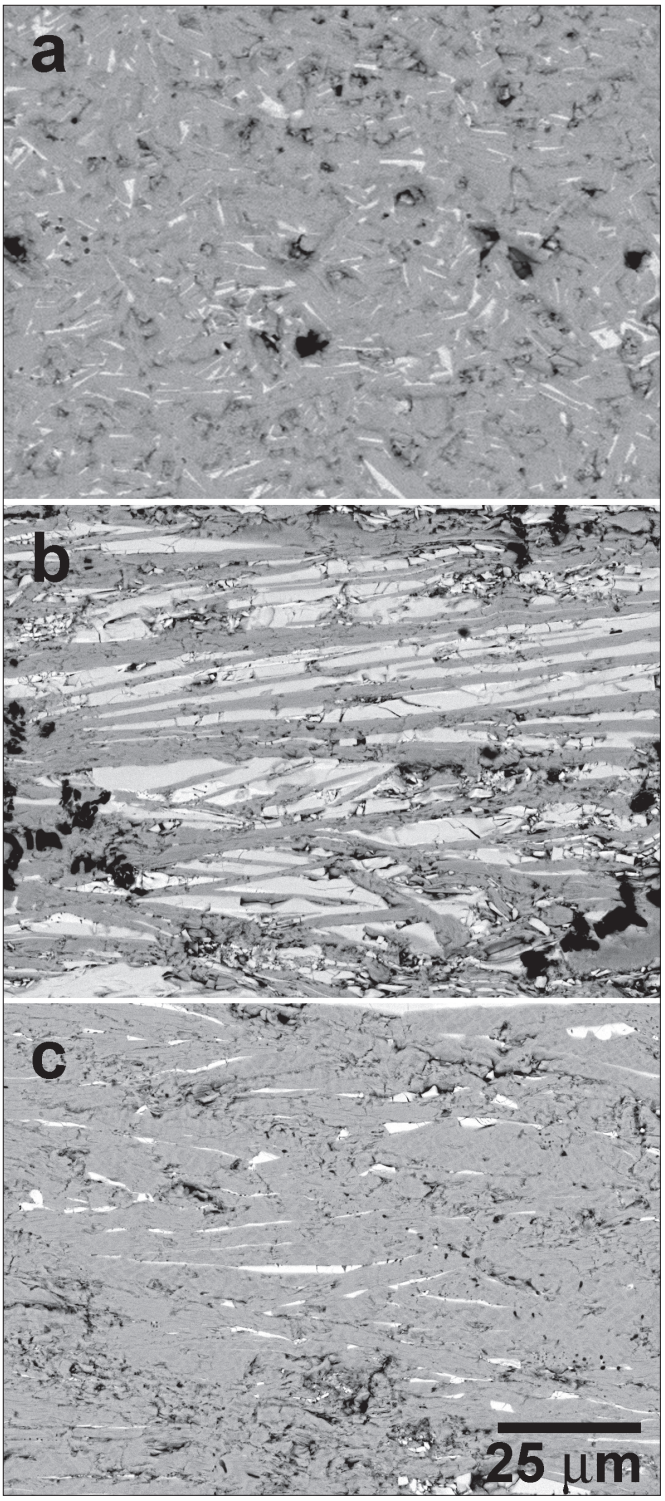

Figure 2. Representative SEM micrographs of longitudinal polished samples a) sintered at 800 ºC for 24 h; b) textured by the LFZ technique; and c) textured by LFZ and annealed at 800 ºC for 24 h. Grey contrast corresponds to the $Bi_2Ca_2Co_{1.7}O_y$ thermoelectric phase, and white and black ones to the $Ca_4Bi_6O_{13}$ and CoO non-thermoelectric secondary phases, respectively.

different phases, which can react to produce the desired one by annealing, as can be seen in Fig. 2c where the annealed textured samples microstructure is illustrated. In the figure, it can be observed that the major phase is the thermoelectric one, with very small amounts of secondary phases. Furthermore, the grain orientation is maintained after the annealing process and the bulk material possess very low porosity (ρ ~ 98 % of the theoretical one).

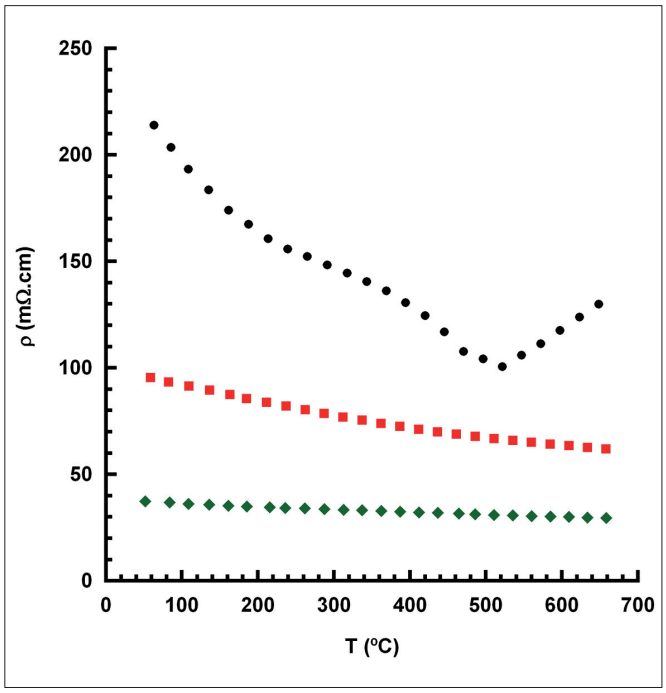

Figure 3. Temperature dependence of the electrical resistivity of $Bi_2Ca_2Co_{1.7}O_x$ samples, as a function of the processing technique. • sintered at 800 ºC for 24 h; ■ textured by the LFZ technique; and ♦ textured-annealed at 800 ºC for 24 h.

The effect of the different processing methods on the thermoelectric properties of these ceramics has been determined by electrical resistivity and Seebeck coefficient measurements. The temperature dependence of the electrical resistivity, as a function of the preparation method, has been measured and represented in Fig. 3. As it can be easily observed in the plot, two different behaviours can be observed, one for the classically sintered samples and another one for the textured samples. The classically prepared materials show a marked semiconducting-like behaviour ($d\rho/dT < 0$) from room temperature to about 550 ºC, changing to a metallic-like one ($d\rho/dT > 0$) at higher temperatures. This is the typical behaviour observed in samples prepared by the classical ceramic method [9]. In the case of the textured samples, they show a slight semiconducting-like behaviour in all the measured temperature range, with lower resistivity values than the obtained for the sintered samples. The evolution of resistivity with the different processing can be explained taking into account the microstructural features discussed previously. As mentioned above, the behaviour of the classically sintered materials is the typical observed in this kind of materials. When they are textured a good grain orientation, together with a decrease on the number of grain boundaries, is produced. In spite of an important raise on the secondary phase content, the resistivity values decrease, indicating that grain orientation and lower amount of grain boundaries influence on the measured resistivity values more than the amount of secondary phases. Moreover, when the as-grown samples are annealed, further decrease on the electrical resistivity is produced by the reduction on the secondary phases´ content. In any case, this decrease is lower than the produced by the texturing process, confirming that the secondary phases affect, in a lower extent than the grain size and orientation, the electrical resistivity values. The lowest resistivity values ~ 30 mΩ.cm at 650 ºC, obtained in the textured-annealed samples, are very similar to the measured in sinter-forged materials at the same temperature (~ 28 mΩ.cm) [30].

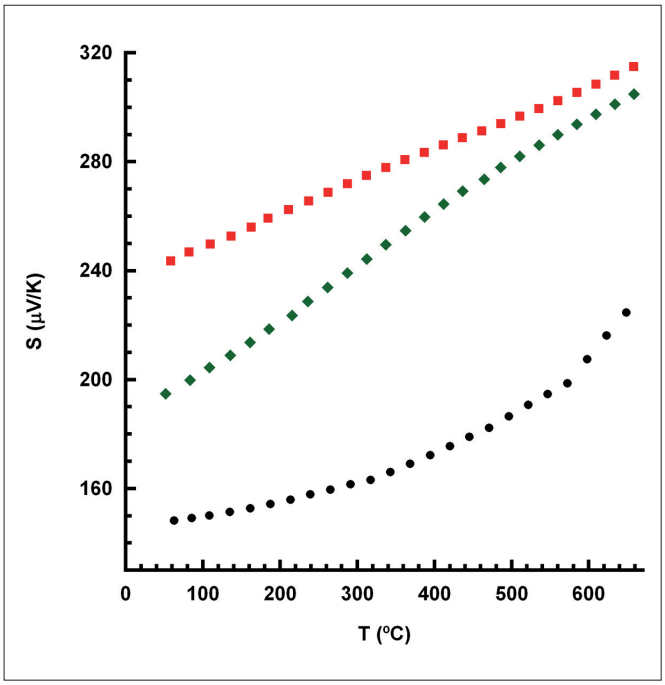

Figure 4. Temperature dependence of the Seebeck coefficient of $Bi_2Ca_2Co_{1.7}O_x$ samples, as a function of the processing technique. • sintered at 800 ºC for 24 h; ■ textured by the LFZ technique; and ♦ textured-annealed at 800 ºC for 24 h.

Fig. 4 displays the Seebeck coefficient variation with temperature, as a function of the processing method. It is evident that the sign of the thermopower is positive for the entire measured temperature range for all the samples which confirms a conduction mechanism mainly governed by holes. In this case, the sintered samples possess lower Seebeck coefficient than the textured samples while the textured-annealed samples show values between them. The very important increase on the Seebeck coefficient values obtained in the as-grown materials is due to the considerable amount of oxygen vacancies produced by this processing method, as reported in previous works [31]. On the other hand, the decrease observed in the Seebeck coefficient when the textured samples are annealed, is in agreement with the results obtained in thermoelectric materials which have shown that at high temperatures oxygen diffuses inside the bulk ceramic material to fill the vacancies, decreasing the Seebeck coefficient values [32]. The highest Seebeck

Bol. Soc. Esp. Ceram. Vidr. Vol 53. 4, 207-212, Julio-Agosto 2014. ISSN 0366-3175. eISSN 2173-0431. http://dx.doi.org/10.3989/cyv.242014

coefficient has been obtained for the as-grown samples at 650 ºC (~ 315 μV/K), much higher than the obtained in sinter-forged materials for 25 h at the same temperature (~ 250 μV/K) [30].

In order to evaluate the thermoelectric performances of these materials, PF has been calculated from the resistivity and Seebeck coefficient values and plotted in Fig. 5. When considering PF values at about 50 ºC (~ room temperature), it can be clearly seen that sintered samples show the lowest values (around 0.01 mW/K²m). The texturing process promotes a very important increase at this temperature, reaching around 0.06 mW/K²m, while the annealing produces further increase until about 0.09 mW/K²m which is around half of the value previously obtained in single crystals (~ 0.18 mW/K²m) [33]. These improvements are produced by the important decrease performed in the electrical resistivity for each process. The maximum measured value at 650 ºC (~ 0.31 mW/K²m) for the annealed samples is nearly 50 % higher than the best obtained in sinter-forged materials for 25 h at the same temperature (~ 0.21 mW/K²m) [30].

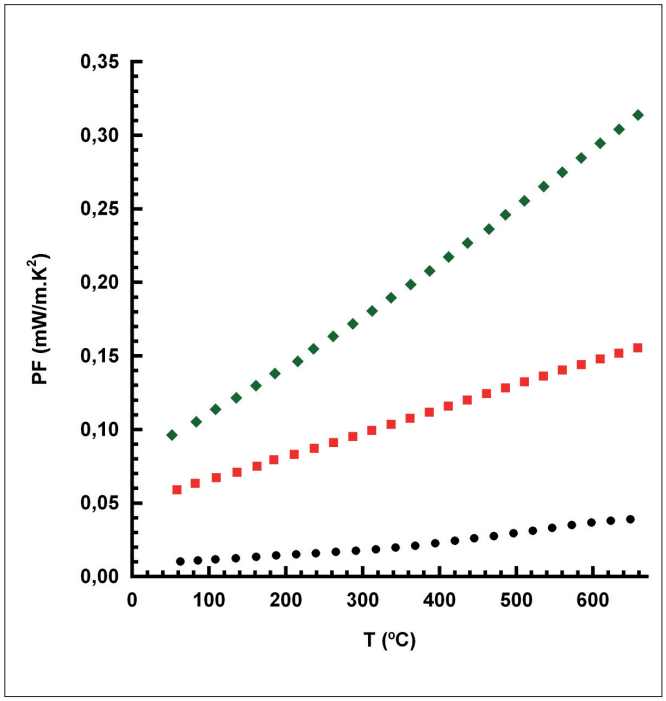

Figure 5. Temperature dependence of the power factor of $Bi_2Ca_2Co_{1.7}O_x$ samples, as a function of the processing technique. • sintered at 800 ºC for 24 h; ■ textured by the LFZ technique; and ♦ textured-annealed at 800 ºC for 24 h.

4. CONCLUSIONS

This paper studies the effect of the processing method on the thermoelectric properties of $Bi_2Ca_2Co_{1.7}O_x$ ceramic materials. The microstructure has shown that samples processed by the classical solid state method are composed of nearly pure $Bi_2Ca_2Co_{1.7}O_x$ phase with randomly oriented grains. On the other hand, LFZ as-grown samples showed well oriented grains with their c-axis nearly perpendicular to the growth direction, together with a relatively high amount of non-thermoelectric secondary phases. Annealing of these samples has produced a very important reduction on the amount of secondary phases. These microstructural changes are reflected on the thermoelectric properties, which increase from the classical solid state prepared samples to the as-grown and the textured-annealed ones. This effect is mainly produced by the decrease on the electrical resistivity of these samples. Maximum PF values at 650 ºC (about 0.31 mW/K²m) are 50 % higher than the best reported in the literature for hot-forging textured materials. All these results show that $Bi_2Ca_2Co_{1.7}O_x$ directionally grown and annealed ceramics are promising materials for practical thermoelectric applications.

ACKNOWLEDGEMENTS

The authors wish to thank the Gobierno de Aragón (Research Groups T12 and T87 for financial support. The technical contributions of C. Estepa and C. Gallego are also acknowledged. Sh. Rasekh acknowledges a JAE-Predoc 2010 grant from CSIC.

REFERENCES

1. Rowe, D.M. (2006): General Principles and Basic Considerations, in Rowe, D.M. (2006) (ed): *Thermoelectrics handbook: macro to nano*. 1st ed. Boca Raton, FL: CRC Press, pp. 1-3–1-7.
2. Mahan, G.; Sales, B.; Sharp, J.; (1997): Thermoelectric materials: New approaches to an old problem, *Phys. Today*, 50: 42–47. http://dx.doi.org/10.1063/1.881752.
3. Naito, H.; Kohsaka, Y.; Cooke, D.; Arashi, H.; (1996): Development of a solar receiver for a high-efficiency thermionic/thermoelectric conversion system, *Sol. Energy*, 58: 191–195. http://dx.doi.org/10.1016/S0038-092X(96)00084-9.
4. Kim, CM.; Hwang, Y.J.; Ryu, Y.H. (2002) US Patent US6393842.
5. Terasaki, I.; Sasago, Y.; Uchinokura, K.; (1997): Large thermoelectric power in $NaCo_2O_4$ single crystals, *Phys. Rev. B.*, 56: 12685–12687. http://dx.doi.org/10.1103/PhysRevB.56.R12685.
6. Sotelo, A.; Constantinescu, G. ; Rasekh, Sh.; Torres, M. A.; Diez, J. C.; Madre, M. A.; (2012): Improvement of thermoelectric properties of $Ca_3Co_4O_9$ using soft chemistry synthetic methods., *J. Eur. Ceram. Soc.*, 32 (10): 2415-2422. http://dx.doi.org/10.1016/j.jeurceramsoc.2012.02.012.
7. Li, F.; Li, J. F.; Li, J. H.; Yao, F. Z.: The effect of Cu substitution on microstructure and thermoelectric properties of $LaCoO_3$ ceramics, *Phys. Chem. Chem. Phys.*, 14: 12213-12220. http://dx.doi.org/10.1039/c2cp41743j.
8. Torres, M. A.; Sotelo, A.; Rasekh, Sh.; Serrano, I.; Constantinescu, G.; Madre, M. A.; Diez, J. C.; (2012): Improvement of thermoelectric properties of $Bi_2Sr_2Co_{1.8}O_x$ through solution synthetic methods, *Bol. Soc. Esp. Ceram. Vidr.*, 51 (1): 1-6. http://dx.doi.org/10.3989/cyv.012012.
9. Sotelo, A.; Rasekh, Sh.; Madre, M. A.; Guilmeau; Marinel, S.; Diez, J. C.; (2011) Solution-based synthesis routes to thermoelectric $Bi_2Ca_2Co_{1.7}O_x$, *J. Eur. Ceram. Soc.*, 31 (9): 1763-1769. http://dx.doi.org/10.1016/j.jeurceramsoc.2011.03.008.
10. Miyazaki, Y.; (2004): Crystal structure and thermoelectric properties of the misfit-layered cobalt oxides, *Solid. State. Ionics*, 172: 463–467. http://dx.doi.org/10.1016/j.ssi.2004.01.046.
11. Maignan, A.; Pelloquin, D.; Hebert, S.; Klein, Y.; Hervieu, M.; (2006): Thermoelectric power in misfit cobaltites ceramics: Optimization by chemical substitutions, *Bol. Soc. Esp. Ceram. Vidr.*, 45 (3): 122-125. http://dx.doi.org/10.3989/cyv.2006.v45.i3.290.
12. Song, X. Y.; Chen, Y.; Chen, S.; Barbero, E.; Thomas, E. L.; Barnes, P.; (2012): Significant enhancement of electrical transport properties of thermoelectric $Ca_3Co_4O_{9+\delta}$ through Yb doping, *Solid. State. Commun.*, 152 (16): 1509-1512. http://dx.doi.org/10.1016/j.ssc.2012.06.014.
13. Rasekh, Sh.; Torres, M. A.; Constantinescu, G.; Madre, M. A.; Diez, J. C.; Sotelo, A.; (2013): Effect of Cu by Co substitution on $Ca_3Co_4O_9$ thermoelectric ceramics, *J. Mater. Sci.: Mater. Electron.*, 24 (7): 2309-2314. http://dx.doi.org/10.1007/s10854-013-1094-5.
14. Sotelo, A.; Rasekh, Sh.; Guilmeau, E.; Madre, M. A.; Torres, M. A.; Marinel, S.; Diez, J. C.: Improved thermoelectric properties in directionally grown $Bi_2Sr_2Co_{1.8}O_y$ ceramics by Pb for Bi substitution, *Mater. Res. Bull.*, 46 (12): 2537-2542. http://dx.doi.org/10.1016/j.materresbull.2011.08.011.

15. Zhang, F. P.; Zhang, X.; Lu, Q. M.; Zhang, J. X.; Liu, Y. Q.; Zhang, G. Z.; (2011): Preparation and high temperature thermoelectric properties of $Ca_{3-x}Ag_xCo_4O_{9+\delta}$ oxides, *Solid. State, Ionics*, 201 (1): 1-5. http://dx.doi.org/10.1016/j.jssc.2010.10.012.
16. Sotelo, A.; Torres, M. A.; Constantinescu, G.; Rasekh, Sh.; Diez, J. C.; Madre, M. A.; (2012): Effect of Ag addition on the mechanical and thermoelectric performances of annealed $Bi_2Sr_2Co_{1.8}O_x$ textured ceramics, *J. Eur. Ceram. Soc.*, 32 (14): 3745-3751. http://dx.doi.org/10.1016/j.jeurceramsoc.2012.05.035.
17. Sun, N.; Dong, S. T.; Zhang, B. B.; Chen, Y. B.; Zhou, J.; Zhang, S. T.; Gu, Z. B.; Yao, S. H.; Chen. Y. F.; (2013): Intrinsically modified thermoelectric performance of alkaline-earth isovalently substituted $[Bi_2AE_2O_4][CoO_2]_y$ single crystals, *J. Appl. Phys.*, 114: 043705. http://dx.doi.org/10.1063/1.4816315.
18. Itahara, H.; Xia, C.; Sugiyama, J.; Tani, T.; (2004): Fabrication of textured thermoelectric layered cobaltites with various rock salt-type layers by using β-$Co(OH)_2$ platelets as reactive templates, *J. Mater. Chem.*, 14 (1): 61-66. http://dx.doi.org/10.1039/b309804d.
19. Noudem, J. G.; Kenfaui, D.; Chateigner, D.; Gomina, M.; (2011): Granular and Lamellar Thermoelectric Oxides Consolidated by Spark Plasma Sintering, *J. Electronic. Mater.*, 40 (5): 1100-1106. http://dx.doi.org/10.1007/s11664-011-1550-z.
20. Sotelo, A.; Guilmeau, E.; Madre, M. A.; Marinel, S.; Diez, J. C.; Prevel, M.; (2007): Fabrication and properties of textured Bi-based cobaltite thermoelectric rods by zone melting, *J. Eur. Ceram. Soc.*, 27 (13-15): 3697-3700. http://dx.doi.org/10.1016/j.jeurceramsoc.2007.02.020.
21. Ferreira, N. M.; Rasekh, Sh.; Costa, F. M.; Madre, M. A.; Sotelo, A.; Diez, J.C.; Torres, M. A.; (2012): New method to improve the grain alignment and performance of thermoelectric ceramics, *Mater. Lett.*, 83: 144-147. http://dx.doi.org/10.1016/j.matlet.2012.05.131.
22. Sotelo, A.; Guilmeau, E.; Madre, M. A.; Marinel, S.; Lemonnier, S.; Diez. J. C.; (2008): $Bi_2Ca_2Co_{1.7}O_x$ thermoelectric ceramics textured by laser floating zone method, *Bol. Soc. Esp. Ceram. Vidr.*, 47 (4): 225-228. http://dx.doi.org/10.3989/cyv.2008.v47.i4.179.
23. Rasekh, Sh.; Madre, M. A.; Sotelo, A.; Guilmeau, E.; Marinel, S.; Diez, J. C.; (2010): Effect of synthetic methods on the thermoelectrical properties of textured $Bi_2Ca_2Co_{1.7}O_x$ ceramics, *Bol. Soc. Esp. Ceram. Vidr.*, 49 (1): 89-94.
24. Diez, J. C.; Rasekh, Sh.; Constantinescu, G.; Madre, M. A.; Torres, M. A.; Sotelo, A.; (2012): Effect of annealing on the thermoelectric properties of directionally grown $Bi_2Sr_2Co_{1.8}O_x$ ceramics, *Ceram. Int.*, 38 (7): 5419-5424. http://dx.doi.org/10.1016/j.ceramint.2012.03.052.
25. Tanaka, Y.; Fujii, T.; Nakanishi, M.; Kusano, Y.; Hashimoto, H.; Ikeda, Y.; Takada, J.; (2007): Systematic study on synthesis and structural, electrical transport and magnetic properties of Pb-substituted Bi–Ca–Co–O misfit-layer cobaltites, *Solid. State. Commun.*, 141 (3): 122-126. http://dx.doi.org/10.1016/j.ssc.2006.10.015.
26. Parise, J. B.; Torardi, C. C.; Whangbo, M.; Rawn, C. J.; Roth, R. S.; Burton, B. P.; (1990): $Ca_4Bi_6O_{13}$, a compound containing an unusually low bismuth coordination number and short Bi–Bi contacts, *Chem. Mater.*, 2 (4): 454-458. http://dx.doi.org/10.1021/cm00010a026.
27. Diez, J. C.; Rasekh, Sh.; Madre, M. A.; Guilmeau, E.; Marinel, S.; Sotelo A.; (2010): Improved thermoelectric properties of Bi-M-Co-O (M = Sr, Ca) misfit compounds by laser directional solidification, *J. Electron. Mater.*, 39 (9): 1601-1605. http://dx.doi.org/10.1007/s11664-010-1232-2.
28. de la Fuente, G. F.; Ruiz, M. T.; Sotelo, A.; Larrea, A.; Navarro, R.; (1993): Microstructure of laser floating-zone (LFZ) textured (Bi-Pb)-Sr-Ca-Cu-O superconductor composites, *Mater. Sci. Eng. A.*, 173 (1-2): 201-204. http://dx.doi.org/10.1016/0921-5093(93)90216-2.
29. Vieira, J. M.; Silva, R. A.; Silva, R. F.; Costa. F. M.; (2013): Enhancement of superconductivity in LFZ-grown BSCCO fibres by steeper axial temperature gradients, *Appl. Surface Sci.*, 258: 9175-9180. http://dx.doi.org/10.1016/j.apsusc.2011.11.054.
30. Guilmeau, E.; Mikami, M.; Funahashi, R.; Chateigner, D.; (2005): Synthesis and thermoelectric properties of $Bi_{2.5}Ca_{2.5}Co_2O_x$ layered cobaltites, *J. Mater. Res.*, 20 (4): 1002-1008. http://dx.doi.org/10.1557/JMR.2005.0131.
31. Constantinescu, G.; Rasekh, Sh.; Torres, M. A.; Madre, M. A.; Diez, J. C.; Sotelo, A.; (2012): Enhancement of the high-temperature thermoelectric performance of $Bi_2Ba_2Co_2O_x$ ceramics, *Scripta Mater.*, 68 (1): 75-78. http://dx.doi.org/10.1016/j.scriptamat.2012.09.014.
32. Madre, M. A.; Costa, F. M.; Ferreira, N. M.; Sotelo, A.; Torres, M. A.; Constantinescu, G.; Rasekh, Sh.; Diez, J. C.; (2013): Preparation of high-performance $Ca_3Co_4O_9$ thermoelectric ceramics produced by a new two-step method, *J. Eur. Ceram. Soc.*, 33 (10): 1747-1754. http://dx.doi.org/10.1016/j.jeurceramsoc.2013.01.029.
33. Kobayashi, W.; Hébert, S.; Muguerra, H.; Grebille, D.; Pelloquin, D.; Maignan, A.; (2008) Thermoelectric properties in the misfit-layered-cobalt oxides [Bi(2)A(2)O(4)] [CoO2](b1/b2) (A=Ca, Sr, Ba, b(1)/b(2)=1.65, 1.82, 1.98) single crystals. *Proceedings ICT 07: Twenty-sixt International Conference on Thermoelectrics*, pp. 117-120.

Recibido: 11/11/2013
Recibida versión corregida: 12/03/2014
Aceptado: 25/03/2014